

Structure-Function Analysis of the Human JC Polyomavirus Establishes the LSTc Pentasaccharide as a Functional Receptor Motif

Ursula Neu,^{1,5} Melissa S. Maginnis,^{2,5} Angelina S. Palma,^{3,6} Luisa J. Ströh,¹ Christian D.S. Nelson,² Ten Feizi,³ Walter J. Atwood,^{2,*} and Thilo Stehle^{1,4,*}

¹Interfaculty Institute for Biochemistry, University of Tübingen, D-72076 Tübingen, Germany

²Department of Molecular Biology, Cell Biology, and Biochemistry, Brown University, Providence, RI 02912, USA

³Glycosciences Laboratory, Faculty of Medicine, Imperial College London, Harrow, Middlesex HA1 3UJ, UK

⁴Department of Pediatrics, Vanderbilt University School of Medicine, Nashville, TN 37232, USA

⁵These authors contributed equally to this work

⁶Present address: REQUIMTE, CQFB, Faculty of Science and Technology/UNL, 2829-516 Caparica, Portugal

*Correspondence: walter_atwood@brown.edu (W.J.A.), thilo.stehle@uni-tuebingen.de (T.S.)

DOI 10.1016/j.chom.2010.09.004

SUMMARY

The human JC polyomavirus (JCV) causes a fatal demyelinating disease, progressive multifocal leukoencephalopathy (PML), in immunocompromised individuals. Current treatment options for PML are inadequate. Sialylated oligosaccharides and the serotonin receptor are known to be necessary for JCV entry, but the molecular interactions underlying JCV attachment remain unknown. Using glycan array screening and viral infectivity assays, we identify a linear sialylated pentasaccharide with the sequence NeuNAc- α 2,6-Gal- β 1,4-GlcNAc- β 1,3-Gal- β 1,4-Glc (LSTc) present on host glycoproteins and glycolipids as a specific JCV recognition motif. The crystal structure of the JCV capsid protein VP1 was solved alone and in complex with LSTc. It reveals extensive interactions with the terminal sialic acid of the LSTc motif and specific recognition of an extended conformation of LSTc. Mutations in the JCV oligosaccharide-binding sites abolish cell attachment, viral spread, and infectivity, further validating the importance of this interaction. Our findings provide a powerful platform for the development of antiviral compounds.

INTRODUCTION

The human JC polyomavirus (JCV) is a member of the Polyomaviridae family, which also includes simian virus 40 (SV40), murine polyomavirus (Polyoma), and the human BK virus (BKV). JCV is a significant human pathogen for which approximately 50%–80% of individuals are seropositive (Kean et al., 2009; Knowles et al., 2003). JCV establishes a persistent, mostly asymptomatic infection in the kidney (Dorries, 1998). However, the virus can become reactivated in immunosuppressed hosts, leading to enhanced viral replication and infection of glial cells, including astrocytes and the myelin-producing oligodendrocytes, in the central nervous system (CNS). JCV infection leads to cytolytic

destruction of oligodendroglia and causes the fatal disease progressive multifocal leukoencephalopathy (PML) (Khalili and White, 2006; Seth et al., 2003; Silverman and Rubinstein, 1965; Zurhein and Chou, 1965). PML is commonly associated with human immunodeficiency virus (HIV) and acquired immunodeficiency syndrome (AIDS) (Cinque et al., 2009). However, the incidence of PML has increased recently in patients receiving immunosuppressive therapies for autoimmune diseases (Carson et al., 2009b; Major, 2009; Van Assche et al., 2005). The prognosis of PML is bleak, as it usually proves fatal within 1 year of symptom onset. Currently there are few treatments for PML (Kishida, 2007).

JCV has a nonenveloped, icosahedral capsid that encloses a circular double-stranded DNA genome (Shah et al., 1996). The major component of the capsid is viral protein 1 (VP1). Structural studies of SV40 and Polyoma virions revealed that polyomavirus capsids consist of 72 VP1 pentamers that are linked via C-terminal extensions of VP1 (Liddington et al., 1991; Stehle et al., 1994). VP1 attaches to receptors on host cells and thereby initiates infection. In crystal structures of Polyoma and SV40 receptor complexes, the receptor binding site is formed by VP1 loops at the outer surface of the capsid (Neu et al., 2008; Stehle et al., 1994). JCV is internalized into cells via clathrin-dependent endocytosis (Pho et al., 2000) and traffics through endosomes and caveosomes (Querbes et al., 2006) to the endoplasmic reticulum (ER). Viral uncoating is thought to begin in the ER, followed by translocation to the cytosol and transport of the genome to the nucleus for viral replication. Previous studies have shown that sialylated oligosaccharides (Dugan et al., 2008; Komagome et al., 2002; Liu et al., 1998b) and the serotonin receptor 5-HT_{2A}R (Elphick et al., 2004) are necessary for JCV entry. The predominant sialic acid in humans is α -5-N-acetyl neuraminic acid (NeuNAc), which caps many different oligosaccharide structures (Varki, 2001).

In this study, we demonstrate that JCV binds specifically to the oligosaccharide lactoseries tetrasaccharide c (LSTc), which contains an α 2,6-linked NeuNAc, using a glycan array screen. The relevance of LSTc as a functional receptor for JCV is confirmed through infectivity assays. We determined the crystal structure of JCV VP1 in complex with LSTc, and based on the structural analysis performed mutagenesis experiments that

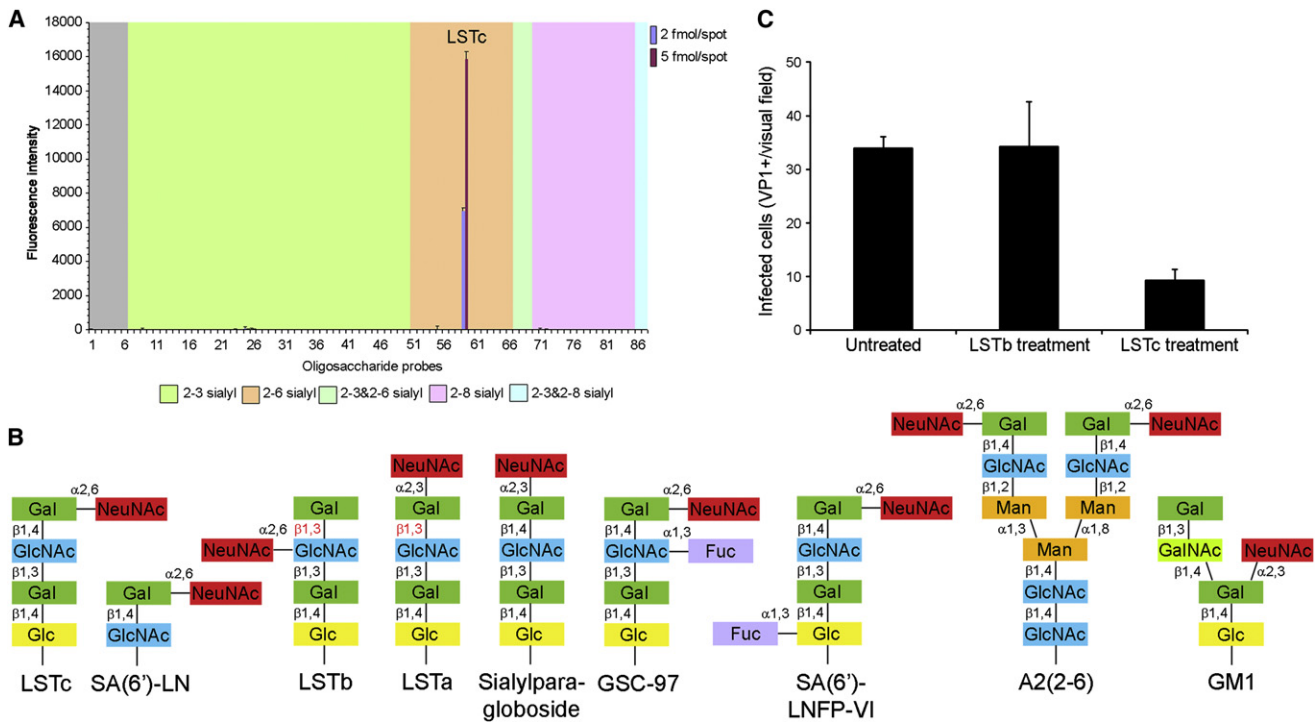


Figure 1. LSTc Is a Functional, Specific Receptor Motif for JCV

(A) Glycan microarray analysis of JCV VP1 showing highly selective binding to LSTc. Numerical scores for the binding intensity are shown as means of fluorescence intensities of duplicate spots at 2 (in blue) and 5 (in red) fmol/spot. Error bars represent half of the difference between the two values.

(B) Structures of selected glycans present on the glycan microarray. The oligosaccharide sequence of the LSTc probe is shown, as well as those of similar compounds that were not bound.

(C) LSTc inhibits JCV infection. JC virus was preincubated with LSTb or LSTc, and complexes were added to SVG-A cells for infection. Infected cells were quantified based on nuclear VP1 staining. The data represent the average number of infected cells per visual field for eight fields of view from an experiment performed in triplicate. Error bars indicate SD of triplicate samples. * $p < 0.05$.

probe the specificity of JCV binding to LSTc. These studies establish the mechanism of JCV cell attachment and provide a foundation for strategies to intervene in the attachment process.

RESULTS

JCV Specifically Engages the Oligosaccharide LSTc

Whereas it is clearly established that JCV infection depends on interaction between VP1 and sialic acid, the nature of the oligosaccharide receptor has remained elusive. To approach this problem, we expressed recombinant JCV VP1 pentamers (Neu et al., 2008; Stehle and Harrison, 1997). The purified pentamers were analyzed on glycan microarrays containing 81 lipid-linked sialylated oligosaccharides differing in the sialyl linkage, backbone sequences, chain lengths, and branching patterns. The microarrays represented carbohydrates found on *N*- and *O*-linked glycoproteins as well as glycolipids (see Table S1 available online). JCV VP1 bound specifically to α 2,6-linked LSTc (Figure 1A). LSTc is a linear pentasaccharide with the sequence NeuNAc- α 2,6-Gal- β 1,4-GlcNAc- β 1,3-Gal- β 1,4-Glc. This sequence represents the type that occurs in the peripheral region of glycans of glycoproteins and glycolipids. The glycan array contained several sequences that closely resembled LSTc, but VP1 did not bind to these (Figures 1A and 1B).

To determine whether JCV engages LSTc to mediate infection of host cells, JCV was preincubated with LSTc, and the mixture was added to SVG-A cells, a glial cell line permissive for JCV. The JCV/LSTc mixture significantly reduced JCV infection, while incubation with JCV/LSTb had no effect on infection (Figure 1C). LSTb is identical to LSTc in molecular weight and composition but features a branching α 2,6-linked sialic acid (Figure 1B). Thus, the specific engagement of an LSTc-like sequence on host cells is critical for JCV infection.

Overall Structure of the JCV VP1-LSTc Complex

We solved the crystal structure of a JCV VP1 pentamer in complex with LSTc at 2.0 Å resolution (Figure 2A, Table 1). The final structure contains amino acids 25–85 and 100–287 for all five VP1 chains. Each VP1 monomer adopts the antiparallel β sandwich fold iconic for viral capsid proteins. Two four-stranded β sheets pack against each other. Their strands are linked by loops in a way that gives rise to a jelly roll topology, with the two β sheets consisting of strands B, I, D, G and C, H, E, F, respectively.

LSTc binds on top of the JCV VP1 pentamer, on the outer surface of the virion (Figures 2A and 2B). Two of the five possible binding sites on VP1 contain LSTc, the other three are occluded by crystal contacts. In the context of cell attachment by an entire

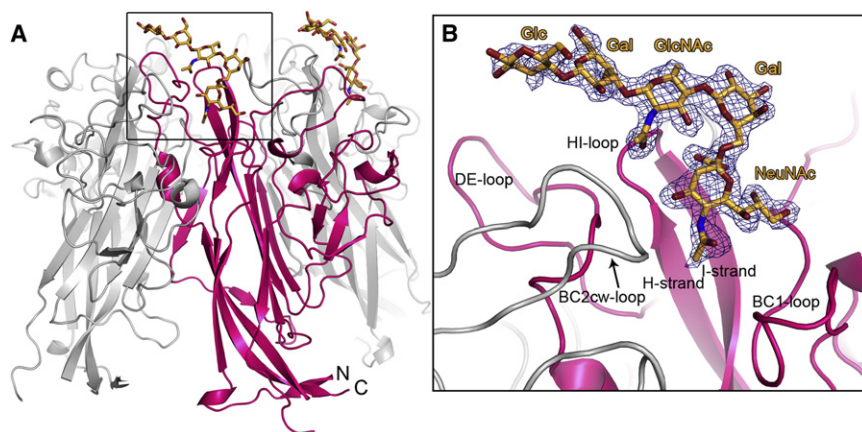


Figure 2. Structure of JCV VP1 in Complex with LSTc

(A) Structure of the JCV VP1 pentamer in complex with LSTc. The protein is shown in cartoon representation, with one VP1 monomer highlighted in pink and the other monomers depicted in gray. The LSTc oligosaccharide is drawn as a stick model and colored according to atom type (nitrogens in blue, oxygens in red, and carbons in orange).

(B) Close-up view of the LSTc binding site. JCV VP1 and LSTc are drawn as in (A). A composite annealed omit difference density map of LSTc is shown contoured at 3.0σ for 2.0 \AA around LSTc.

virion, however, all five binding sites on a given pentamer could be occupied by LSTc, which is not unlikely, given the relatively low affinity of a single protein-carbohydrate interaction. The binding site is formed by residues from the BC, DE, and HI loops from one monomer as well as the BC loop from its clockwise neighbor (Figure 2B). These loops also engage receptors in SV40 and Polyoma VP1, and they are the only parts of VP1 that differ significantly among the three viruses (Neu et al., 2008; Stehle and Harrison, 1997). The extensive BC loop can be subdivided into two parts facing in different directions (BC1 and BC2). LSTc binds where the BC1 loop of one monomer

approaches the tip of the BC2 loop of its clockwise neighbor, and it interacts with both. For reasons of clarity, residues and loops of the main binding VP1 monomer will not be specifically labeled, while those of its clockwise and counterclockwise neighbors will be designated cw and ccw, respectively, herein.

Interactions of JCV VP1 with LSTc

The bound LSTc molecule resembles the letter “L,” with the shorter leg formed by NeuNAc and its $\alpha 2,6$ -linkage to Gal, and the longer leg consisting of the GlcNAc- $\beta 1,3$ -Gal- $\beta 1,4$ -Glc trisaccharide (Figure 2B). In solution, the glycosidic bonds of LSTc can rotate freely due to its unbranched sequence, and the molecule can assume different conformations (Breg et al., 1989). However, as the NeuNAc and GlcNAc moieties of LSTc are attached to positions 6 and 1 of the same Gal residue, all conformations feature a kink. JCV VP1 interacts selectively with one of these conformations, contacting sugar moieties in both legs of the L-shaped ligand. The observed conformation of LSTc as well as its orientation with respect to the VP1 surface differs from previously published homology models of JCV interactions with oligosaccharides (Gee et al., 2004; Sunyaev et al., 2009). These homology models were based on interactions observed in the structure of Polyoma VP1 in complex with an $\alpha 2,3$ -sialylated oligosaccharide (Stehle and Harrison, 1997). Although NeuNAc is bound in a similar location at the outer surface of both proteins, the orientation of NeuNAc with respect to the protein surface is different, and the interactions with the oligosaccharide structures are not conserved.

Most of the interactions between JCV and LSTc involve the three longer functional groups projecting from the terminal NeuNAc residue (Figures 3A and 3B). The NeuNAc carboxylate faces toward the HI loop and is recognized by parallel hydrogen bonds to the side chains of S266 and S268, as well as a water-mediated hydrogen bond to S266. The extended NeuNAc glycerol chain docks into a shallow depression on the protein surface that is shaped by residues in the BC and HI loops. The bottom of the depression is formed by the side chain of Q270. Hydrogen bonds to the amide and hydroxyl groups of S60, located at the rim of the depression, further anchor the glycerol chain. The methyl moiety of the *N*-acetyl group inserts into a hydrophobic cavity at the intersection between the HI, BC1, and BC2cw loops. The

Table 1. Crystallographic Statistics of JCV VP1 and JCV VP1-LSTc Structures

	JCV VP1-LSTc Complex		JCV VP1	
Data Collection				
Unit cell (\AA)	149.7, 96.3, 128.2		149.6, 96.0, 128.6	
Unit cell ($^\circ$)	90, 110.3, 90		90, 110.4, 90	
Space group	C2		C2	
Resolution (\AA)	35–2.0	2.05–2.00	20–1.95	2.00–1.95
Total reflections	437,707	30,603	419,669	15,867
Unique reflections	114,938	8,302	119,853	8,429
I/ σ I	9.6	2.7	10.9	2.5
R _{merge} (%)	11.7	48.3	9.3	32.4
Completeness (%)	99.5	97.5	96.5	91.7
Structure Refinement				
Protein atoms	10,200		10,135	
Average B factor (\AA^2)	16.6		15.7	
Carbohydrate atoms	136		-	
Average B factor (\AA^2)	24.3		-	
Solvent atoms	980		1,054	
Average B factor (\AA^2)	25.4		26.4	
R _{work} (%)	18.9		18.0	
R _{free} (%)	21.2		20.8	
Rmsd bond lengths [\AA]	0.006		0.007	
Rmsd bond angles ($^\circ$)	0.9		1.0	

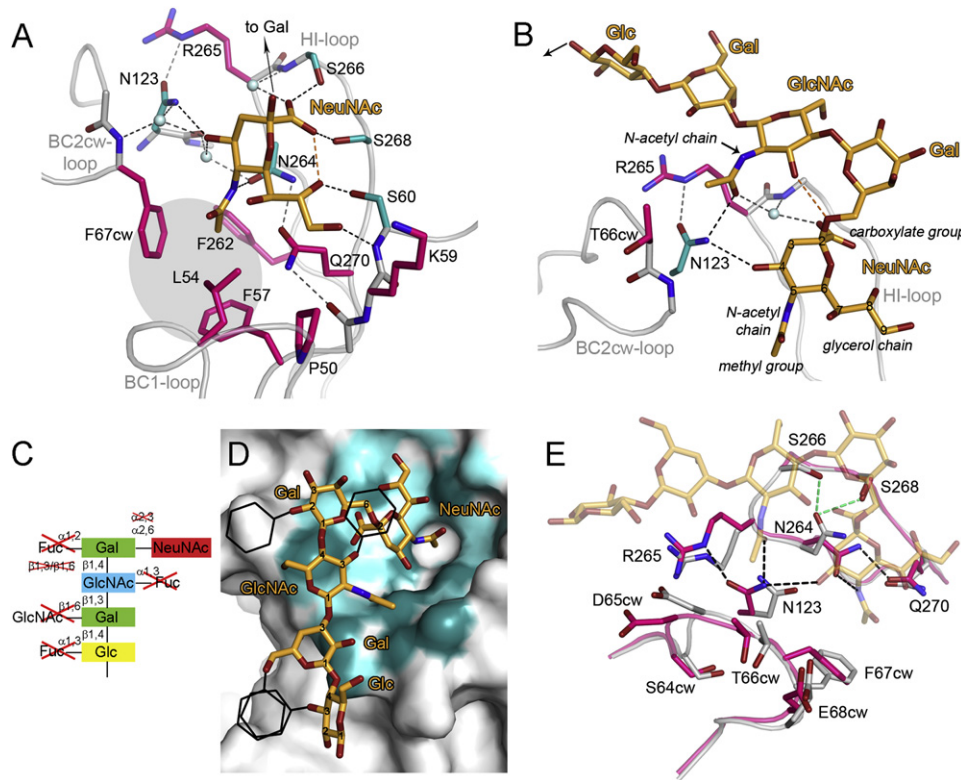


Figure 3. Interactions between JCV VP1 and LSTc

(A) Interactions between JCV VP1 and the terminal NeuNAc of LSTc. JCV VP1 is shown as a cartoon, with side chains interacting with LSTc in stick representation. Waters are represented with spheres. Residues forming direct hydrogen bonds to NeuNAc are colored teal and residues forming van der Waals contacts or water-mediated hydrogen bonds are colored pink. Direct hydrogen bonds between JCV VP1 and NeuNAc are shown as black dashed lines, and water-mediated hydrogen bonds or bonds between protein atoms are colored gray. Intramolecular hydrogen bonds within the oligosaccharide are orange.

(B) Interactions between JCV VP1 and other parts of LSTc.

(C) The cartoon represents structural features of oligosaccharides that are required for JCV binding. These were extracted from our glycan microarray data. Crossed-out sugar residues would produce steric clashes.

(D) Structural basis for JCV VP1 specificity for LSTc. JCV is shown in surface representation, with residues interacting with LSTc colored according to their change in surface accessibility upon LSTc binding (gray <math><1 \text{ \AA}^2</math> change, light teal 1–10 $\text{\AA}^2</math> change, dark teal >10 $\text{\AA}^2</math> change). The branching substitutions at LSTc that abolish binding are indicated as black hexagons, indicating where they would clash with protein or LSTc atoms.$$

(E) Structural changes in JCV VP1 upon LSTc binding. The structures of unliganded (gray) and liganded (pink) JCV VP1 were superposed using the β sandwich core residues. Hydrogen bonds only present in unliganded VP1 are indicated with green dashes, and those only present in the complex are colored black.

N-acetyl group is hydrogen bonded to the side chain of N264. Finally, the O4 hydroxyl group of NeuNAc forms a hydrogen bond with the side chain of N123. The O4 hydroxyl group also makes two water-mediated hydrogen bonds to N123 and F67cw.

Specific contacts between JCV VP1 and the long leg of the L-shaped LSTc mostly involve the GlcNAc residue. The side chain of N123 forms hydrogen bonds to both the carbonyl of the GlcNAc *N*-acetyl group and the side chain of R265. In turn, the carbonyl group of the *N*-acetyl chain forms water-mediated hydrogen bonds with S266 and the carboxyl group of the NeuNAc residue. The methyl group of the GlcNAc *N*-acetyl chain makes van der Waals interactions with the methyl group of T66cw. In addition, there is a hydrogen bond within LSTc linking GlcNAc with the glycosidic oxygen of Gal.

Interestingly, 6-sialyl-lactosamine, which like LSTc has a NeuNAc- α 2,6-Gal- β 1,4-GlcNAc motif, was not recognized by JCV VP1. Since the oligosaccharide is directly linked to a lipid tag

(Table S1), productive engagement of this compound might be prevented because the GlcNAc group, which contributes contacts in the case of LSTc, is in close proximity to the lipid here. Thus, for reasons of accessibility, JCV requires at least the LSTc pentasaccharide as a binding motif (Figure 3C). The glycan array tested the effect of additional, branching residues to this minimal binding motif. Attachment of a fucose to O3 of GlcNAc and O3 of Glc, or attachment of a branching oligosaccharide chain to O6 of Gal (probe 64, Figure 1A, Table S1), would lead to clashes with either JCV VP1 or other LSTc residues (Figure 3D). Attachment of a fucose to O2 of the first Gal does not occur in parallel with sialylation of that group. However, the presence of a GlcNAc residue instead of the terminal Glc of LSTc, as present in most glycans carrying LSTc-like sequences, is unlikely to alter the conformation of the oligosaccharide.

There are no hydrogen bonds between JCV VP1 and the remaining three sugar moieties in LSTc. However, the Glc and two Gal residues contribute to the surface area buried upon

complex formation (Figure 3D) and are well-ordered in the structure, indicating low flexibility due to van der Waals interactions with VP1. These interactions are clearly relevant for affinity and specific binding of JCV, as demonstrated by the glycan microarray.

JCV VP1 Undergoes Induced-Fit Movements upon Binding LSTc

To determine whether JCV VP1 undergoes conformational changes upon ligand binding, we solved the structure of unliganded JCV VP1 at 1.95 Å resolution (Table 1). Comparison with liganded VP1 shows that residues in the binding site rearrange upon ligand binding (Figure 3E). In the unliganded structure, the N264 side chain is oriented toward the side chains of S266 and S268 and forms hydrogen bonds with both residues. Upon ligand binding, N264 swings around to interact with Q270 and the *N*-acetyl chain of NeuNAc. In the unliganded structure, the “binding” conformation of N264 is already present as a second conformation, suggesting a dynamic equilibrium between two conformations that is shifted by ligand binding.

More drastic changes are seen at residue N123, whose hydrogen bonds are critical for recognizing the L-shaped binding conformation of LSTc. In the absence of LSTc, the N123 side chain points closer toward the NeuNAc binding site, and would clash with NeuNAc. To accommodate NeuNAc, the N123 side chain moves. Its altered position leads to clashes with main-chain atoms in the BC2cw loop, and so residues 64–68 of the BC2cw loop move to accommodate the new conformation of N123. Induced-fit movements were not observed in receptor interactions of SV40 and Polyoma (Neu et al., 2008; Stehle and Harrison, 1997). The induced fit of JCV VP1 may facilitate binding to LSTc in a specific conformation.

Carbohydrate Binding Sites in VP1 Are Necessary for JCV Attachment, Infection, and Spread

The crystal structure of VP1 in complex with LSTc revealed numerous contacts between the protein and LSTc. To test whether binding of LSTc is required for JCV infection, we introduced point mutations in the oligosaccharide-binding sites of VP1 into an infectious JCV clone (highlighted in Figure 4A). One set of mutants was designed to abolish the interaction with NeuNAc, either by removal of hydrogen bonds (S266A/S268A) or by steric hindrance (S266N/S268N and L54Y). We also probed the importance of N123, which undergoes induced-fit movements to specifically recognize the L-shaped conformation of LSTc, by mutating it to alanine. In addition, we mutated A126 and R265 in a unique groove on the VP1 surface (Figure 4A), which is not present in Polyoma and SV40 (Neu et al., 2008; Stehle et al., 1994) and may be relevant for interactions with JCV cell surface receptors. In addition, R265 forms van der Waals contacts with the long leg of LSTc. Mutants were analyzed for infectious spread in long-term growth assays (Figures 4B and 4D). On the final day of the growth assay, supernatants were harvested and used to inoculate SVG-A cells for an infectivity assay (Figures 4C and 4E). Mutation of residues in the NeuNAc binding site (L54Y, S266A/S268A, and S266N/S268N) completely abolished JCV spread and infectivity (Figures 4B and 4C). Interactions mediated by each of these residues must therefore be required for a productive interaction with sialic

acid, which in turn is essential for JCV growth. N123A had delayed viral spread in culture compared to wild-type (Figure 4D) and exhibited a 50% reduction in infectivity (Figure 4E), demonstrating the important role of N123 in accommodating LSTc. Mutation of R265, which forms van der Waals contacts with LSTc, did not affect growth and infectivity but resulted in reduced binding (Figure 4F). Virus with a mutation in the groove (A126Q) was capable of infection, and grew to levels equivalent to wild-type JCV. This indicates that, while the groove is unique to JCV VP1, residue A126 likely does not contribute to receptor binding. Virus carrying the more drastic A126Y mutation was unable to grow. We envisage that this mutation introduces local structural changes that affect residues critical for sialic acid binding.

The residues targeted for mutation are far from the VP1 regions that mediate capsid assembly or interact with minor capsid proteins. In order to verify that the mutants do not alter or destabilize the structure of VP1, we introduced the mutations into the pentamer expression construct and expressed mutant proteins in *E. coli*. Like wild-type, all mutant proteins were purified as pentamers, indicating that they are properly folded (Figure S1A). Circular dichroism spectroscopy experiments confirm that secondary structure compositions of wild-type and mutant proteins are identical (Figure S1B).

To determine whether the decrease in viral growth and infectivity exhibited by mutant viruses was attributable to virus binding, we analyzed wild-type and mutant JCV VP1 pentamers in a flow cytometry-based cell-binding assay (Figure 4F). Purified pentamers were incubated with SVG-A cells, and binding was detected using an antibody specific for their His tag. Flow cytometry analysis revealed that mutants that do not support infection (L54Y, A126Y, S266A/S268A and S266N/S268N) or do so at reduced levels (N123A) also have reduced binding to cells in comparison to wild-type VP1. Mutants with wild-type-like growth properties (A126Q, R265A) were capable of binding to host cells. While A126Q bound similar to wild-type, R265A exhibits reduced binding. As the R265 side chain forms van der Waals contacts with LSTc (Figures 3 and 4), its mutation likely results in a modest reduction of affinity that can be compensated by avidity in the context of the virion and thus does not affect viral growth and infectivity. These data demonstrate that the specific contacts between JCV VP1 and LSTc observed in the crystal structure play a critical role in JCV attachment and infection.

Structural Basis for the Binding Specificity of JCV

The crystal structure provides a platform for understanding the binding properties of JCV VP1 to host cells. Comparison with the structure of SV40 VP1 in complex with its receptor GM1, which carries an α 2,3-linked NeuNAc at a branching point (Figure 1B), reveals that JCV and SV40 bind terminal NeuNAc at the same location in the VP1 pentamer (Neu et al., 2008). The specific interactions with the functional groups of NeuNAc are conserved (Figure 5), highlighting their importance.

However, the JCV and SV40 VP1 proteins differ at the cavity into which the methyl group of the terminal NeuNAc inserts. In SV40 VP1, this cavity is quite large, polar at its rim, and likely water filled, while the cavity is smaller and more hydrophobic in JCV. This reflects the different host organisms of the two viruses.

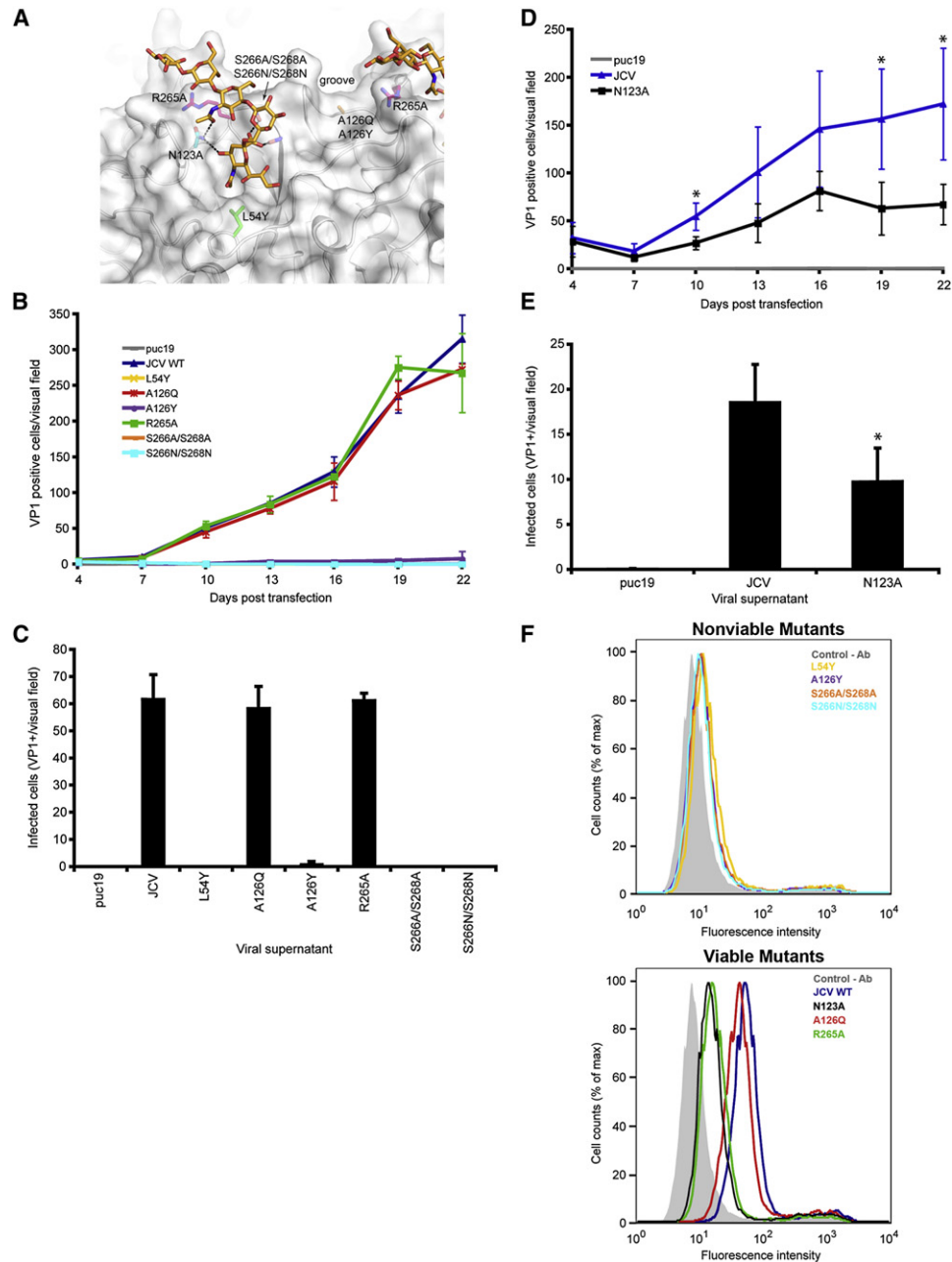


Figure 4. Growth, Infectivity, and Binding of JCV VP1 Mutants

(A) Point mutations introduced into JCV VP1. LSTc is shown in stick representation.

(B) Growth of JCV VP1 wild-type and mutant viruses. SVG-A cells were transfected with linearized DNA from JCV VP1 wild-type and mutant constructs. Transfected cells were fixed and stained at day 4 posttransfection, then at 3 day intervals for 22 days by indirect immunofluorescence. Transfected or infected cells were quantified based on nuclear VP1 staining. Each data point represents the average number of infected cells per visual field for ten fields of view for three independent experiments. Error bars indicate SD.

(C) Infectivity of supernatants from JCV VP1 wild-type and mutant viruses. SVG-A cells were inoculated with supernatants harvested from infected cells at day 22 from (B). Cells were fixed and stained by indirect immunofluorescence at 72 hr postinfection and quantified based on nuclear VP1 staining. The results are presented as the average number of infected cells per visual field for ten visual fields from three individual samples performed in triplicate. Error bars indicate SD.

(D) Growth of JCV VP1 wild-type and N123A. N123A was analyzed for viral growth as in (B). Each data point represents the average of number of infected cells per visual field for ten fields of view for three independent experiments. Error bars indicate SD. *p < 0.05.

(E) Infectivity of supernatants from JCV VP1 wild-type and N123A. N123A was analyzed for infectivity as in (C). Error bars indicate SD. *p < 0.05.

(F) Cell-binding analysis of JCV wild-type and mutant pentamers. SVG-A cells were incubated with His-tagged wild-type or mutant pentamers and a Penta His Alexa Fluor 488 antibody. Cells were fixed and pentamer binding was analyzed by flow cytometry. Histograms represent the fluorescence intensity of Alexa 488 for antibody alone (filled) and pentamer samples (open) for 10,000 gated events. Data are grouped into two histograms based on mutants that propagate (bottom) or do not propagate (top) in SVG-A cells.

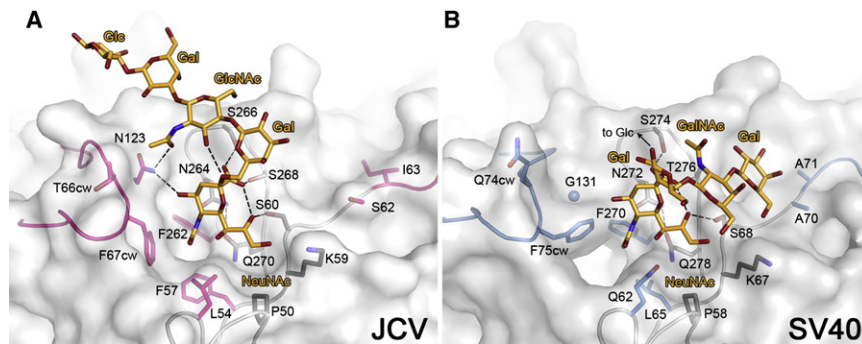


Figure 5. Comparison of Oligosaccharide Binding Sites of JCV and SV40 VP1

(A) JCV VP1 in complex with LSTc. (B) SV40 VP1 in complex with GM1. The Glc in GM1 does not contact the protein and was omitted for clarity. The proteins are shown in surface representation, with the BC and HI loops also indicated in cartoon representation. Residues contributing to ligand binding or specificity are shown in stick representation. They are colored gray when they are in the same conformation in the two proteins. Residues that are not conserved and assume different conformations are colored pink for JCV and blue for SV40. A blue sphere indicates the C α position of G131 in SV40. The carbohydrate ligands are shown as orange sticks. Key hydrogen bonds are shown as black dashes.

In simians, the natural hosts of SV40, the predominant sialic acid is not NeuNAc but *N*-glycolyl neuraminic acid (NeuNGc), which carries the larger and more polar CH₂-OH group instead of the methyl group of NeuNAc (Varki, 2001). SV40 binds to NeuNGc-GM1 better than to NeuNAc-GM1 (Campanero-Rhodes et al., 2007), which is consistent with its larger, more polar cavity. However, NeuNAc is the most abundant sialic acid in humans, and the smaller and more hydrophobic cavity of JCV is consistent with its preference of NeuNAc-LSTc over NeuNGc-LSTc. Thus, the structure of the oligosaccharide binding site has consequences for the species specificity of the virus.

The position of NeuNAc in the larger context of an oligosaccharide is clearly a major determinant of specificity (Figures 3C and 3D). Amino acid N123 is key to recognizing the observed L-shaped conformation of LSTc, since it makes hydrogen bonds with both the GlcNAc and terminal NeuNAc sugar residues (Figures 3A and 3B). Different linkages of NeuNAc, Gal, and GlcNAc would not produce the precise arrangement of NeuNAc and GlcNAc that is required for complex formation. As a result, sialylparagloboside, which carries α 2,3-linked NeuNAc but is otherwise identical in sequence to LSTc, is not recognized (Figure 1). The residue corresponding to N123 in SV40 is a glycine, which would not be able to mediate these contacts (Figure 5), explaining why SV40 does not attach to sequences terminating in NeuNAc- α 2,6-Gal- β 1,4-GlcNAc (Campanero-Rhodes et al., 2007; Neu et al., 2008).

Our data therefore provide strong support for a mode of binding that requires both a terminal NeuNAc and the extended L-shaped binding conformation of LSTc in the context of a long, linear chain.

DISCUSSION

We demonstrate here by glycan array screening that recombinant JCV VP1 pentamers selectively bind the LSTc oligosaccharide. The observed interaction is of physiologic relevance, as JCV infection can be blocked specifically by incubation with soluble LSTc. In order to understand the molecular basis for this recognition, we determined the structure of the JCV capsid protein, VP1, in complex with LSTc at 2.0 Å resolution. The structure shows that JCV engages both the terminal sialic acid and the unique L-shaped conformation of LSTc, which results in additional contacts of the GlcNAc moiety with VP1 and likely is

a key determinant of its interaction with JCV VP1. Mutagenesis of residues involved in sialic acid binding results in viruses that are unable to grow and infect due to a binding defect.

Our finding that glycans terminating in the LSTc motif serve as main receptors for JCV is consistent with biochemical assays involving natively glycosylated cells (Liu et al., 1998b) (Figure 1B). Homologs of LSTc, in which a GlcNAc replaces the terminal Glc, are present in the human body as the termini of long oligosaccharide chains of the “i” antigen type (Feizi, 1985). All of the glycans terminating in GlcNAc-LSTc contain repeating units of [3-Gal- β 1,4-GlcNAc- β 1-]_n (polyLacNAc repeats), and fulfill the steric condition of a long carbohydrate that is unbranched at its tip. These compounds should therefore bind JCV. The i antigen is expressed on a high proportion of human peripheral lymphocytes (Feizi et al., 1980). Glycan profiling by mass spectrometry has identified long glycans consistent with the LSTc motif in the *N*-glycan fractions of several human tissues including kidney, lung, and spleen (<http://www.functionalglycomics.org/>), but tissues of the entire CNS were not analyzed. Lectin staining of human tissues revealed that α 2,6-linked NeuNAc is present on the surface of B lymphocytes of the tonsils and spleen, on kidney and lung cells, as well as on astrocytes and oligodendrocytes (Eash et al., 2004). Only very low-level lectin staining was seen for neurons and T lymphocytes. Notably, neurons, which express the serotonin receptor, are not susceptible to infection with JCV, most likely because they lack the oligosaccharide receptor. As the expression pattern of LSTc-carrying glycans corresponds to sites of JCV persistence (the kidney), and pathogenesis (the glial cells of the CNS), it is likely that the observed specificity of JCV for LSTc contributes to targeting the virus to these sites.

Previous studies report that JCV was also able to use α 2,3-linked sialic acids as receptors (Dugan et al., 2008). It is possible that our glycan microarrays performed with pentamers failed to detect low-affinity interactions of JCV with α 2,3-linked compounds because pentamers bind with much lower avidity than virions. However, given the strong signal observed for LSTc, such interactions would be very weak. Inspection of the structure shows that linear α 2,3-linked compounds would not be able to interact favorably with JCV VP1. However, branched compounds such as GM1 and GM2 would be able to bind, albeit with significantly lower affinity compared to LSTc because of their much smaller contact areas. Interestingly, unpublished

results by Leonid Gorelik and the Consortium for Functional Glycomics (CFG), which are available online at <http://www.functionalglycomics.org/> according to CFG policy, confirm these predictions. In glycan array screens of JCV VLPs of Mad-1 (which has the same VP1 as the strain used in our studies), strong binding was observed to LSTc-containing sequences, and weak binding was observed for GM2, GM1, and similar short, branched, α 2,3-linked sequences. The weaker interactions with GM1 and GM2 would not appear to be functional because SV40, which does use GM1 as a receptor, does not compete with JCV for binding sites (Liu et al., 1998a).

In contrast to the related polyomaviruses SV40, Polyoma, and BKV, JCV does not enter cells by cholesterol-dependent endocytosis but instead uses clathrin-mediated endocytosis. It is enticing to speculate that this difference is reflected by their carbohydrate receptor specificities. SV40, Polyoma, and BKV all use gangliosides (Low et al., 2006; Tsai et al., 2003), which in the case of SV40 initiate entry by inducing curvature of the plasma membrane (Ewers et al., 2010). To induce curvature upon binding, the oligosaccharide portion of the receptor must be relatively rigid, which is the case for short, branched gangliosides (Acquotti et al., 1991), but not for long, flexible polyLacNAc extensions. Thus, the few amino acid changes between JCV and related polyomaviruses might not only determine receptor specificity but also target the virus to a different entry pathway.

Statistical analyses of JCV sequences demonstrate that 52% of PML patients carry JCV with one mutation in VP1 (L54F, K59M/E/N, N264D/T, S266F/L, or S268F/Y/C) that likely arose from positive selection (Sunyaev et al., 2009). Residues L54, N264, S266, and S268 mediate direct contacts with NeuNAc. Mutation of any of these four residues therefore adversely affects sialic acid binding (Figures 3A and 4). Consistently, the L54F and S268F mutants have reduced hemagglutination activity (Sunyaev et al., 2009). Although residue K59 also contacts NeuNAc, its replacement with M, E, or N would still allow for similar contacts. Not all of the mutations can therefore be attributed to a selective pressure on the virus to alter its receptor binding site.

It is interesting to speculate about how mutations that should block LSTc binding would be selected for in individuals with PML. It is conceivable that JCV featuring a mutated oligosaccharide binding site can spread more rapidly to the CNS from its site of persistence in the kidney because of diminished attachment to carbohydrates. This scenario would be similar to a point mutation in Polyoma VP1 that abolishes binding to nonfunctional pseudoreceptors, thereby increasing viral spread and rendering the virus more pathogenic (Freund et al., 1991). However, a defect in sialic acid binding would abolish engagement of both LSTc-carrying glycans and branched α 2,3-linked compounds. Unpublished glycan array screening data by Leonid Gorelik and the CFG confirms this (<http://www.functionalglycomics.org/>). One also cannot ascertain whether JCV develops mutations in VP1 while replicating in remote sites of infection such as the kidney or if they develop in the brain. Moreover, it is not clear if patients carrying mutant JCV also carry wild-type JCV. Finally, viruses with the mutations L54Y, S266A/S268A, and S266N/S268N in the sialic acid binding site were unable to infect cells and propagate in a long-term growth assay because of a cell binding defect (Figure 4). Since we mutated the residues identified in PML patients, albeit to different amino

acids, we would predict that the mutations present in PML patients would not propagate efficiently in glial cells.

In recent years, the incidence of PML has increased beyond the HIV/AIDS population to include patients undergoing immunosuppressive therapies for immunological disorders such as multiple sclerosis (Linda et al., 2009; Wenning et al., 2009), Crohn's disease (Van Assche et al., 2005), rheumatoid arthritis, and systemic lupus erythematosus (Carson et al., 2009a). Treatment options for PML are currently inadequate (Kishida, 2007), especially given the rapid devastation of this disease. We expect that knowledge about the structure of JCV VP1 and its interaction with receptors can serve as a platform from which such treatment strategies can be developed.

EXPERIMENTAL PROCEDURES

Protein Expression and Purification

cDNA coding for amino acids 22–289 of the Mad-1 strain of JCV VP1 was cloned into the pET15b expression vector (Novagen) in frame with an N-terminal hexahistidine tag (His tag) and a thrombin cleavage site. The N-terminal truncation was made because presence of these amino acids had inhibited crystallization of the homologous Polyoma VP1, while the C-terminal truncation was made to prevent capsid assembly in crystallization setups (Stehle and Harrison, 1997). Mutations were introduced using Phusion mutagenesis (NEB) according to the manufacturer's instructions and confirmed by sequencing (Table S2). Proteins were overexpressed in *E. coli* BL21(DE3) and purified using nickel affinity chromatography. For glycan array screening, flow cytometry, and circular dichroism, the proteins were additionally purified by gel filtration. For crystallization, the His tag was removed by incubation with thrombin prior to gel filtration. After cleavage, the nonnative amino acid sequence GSHM remains at the N terminus of VP1.

Glycan Array Screening

The microarray was composed of 87 sequence-defined lipid-linked oligosaccharide probes: 81 sialyl-terminating probes and six neutral probes as negative controls (Table S1). The probes were robotically printed in duplicate on nitrocellulose-coated glass slides at 2 and 5 fmol per spot using a noncontact instrument (Palma et al., 2006). The protein was precomplexed with mouse monoclonal anti-poly-histidine (Ab1) and biotinylated anti-mouse IgG antibodies (Ab2) (both from Sigma) in a ratio of 4:2:1 (by weight). In brief, the JCV VP1-His tagged protein-antibody precomplexes were prepared by preincubating Ab1 with Ab2 for 15 min at ambient temperature, followed by addition of VP1 and incubation for a further 15 min on ice. The VP1-antibody complexes were diluted in 5 mM HEPES (pH 7.4), 150 mM NaCl, 0.3% (v/v) Blocker Casein (Pierce), 0.3% (w/v) bovine serum albumin (Sigma), 2.5 mM DTT, and 5 mM CaCl₂ to give a final VP1 concentration of 150 μ g/ml, and overlaid onto the arrays at 20°C for 2 hr. Binding was detected with Alexa Fluor 647-labeled streptavidin (Molecular Probes) and imaging (Palma et al., 2006), and data analysis (Stoll and Feizi, 2009) was as described.

Crystallization and Data Collection

JCV VP1 was concentrated to 4.5 mg/mL and crystallized by sitting drop vapor diffusion at 20°C. The reservoir solution contained 12% (w/v) PEG 3,350, 0.1 M HEPES (pH 7.5), and 0.2 M KSCN. Drops were set up by mixing 1 μ l protein solution with 1 μ l reservoir solution and 0.2 μ l microseeding stock from previously obtained crystals. Crystals were harvested into a solution containing 10% PEG 3,350, 0.1 M HEPES (pH 7.5), and 0.2 M KSCN and cryoprotected by soaking for 10 s in harvesting solution containing 30% (v/v) glycerol and flash freezing in liquid nitrogen. For complex formation, crystals were soaked for 3 min in harvesting solution supplemented with 5 mM LSTc oligosaccharide. The cryoprotecting solution also contained the same concentration of LSTc oligosaccharide.

Structure Determination

Data reduction was performed with XDS (Kabsch, 2010), and the structure was solved by molecular replacement in Phaser (McCoy et al., 2007) using a search

model generated from the SV40 VP1 pentamer structure (3BWQ). Refinement was then performed with Phenix and Refmac5 (Adams et al., 2010; Murshudov et al., 1997), and model building was done in Coot (Emsley and Cowtan, 2004). Five-fold noncrystallographic symmetry restraints were used throughout the refinement for most of the protein. In data from crystals soaked in LSTc, the ligand was located in $2F_o - F_c$ and $F_o - F_c$ weighted electron density maps. The ligand was refined using restraints from the CCP4 library, with the exception of the $\alpha 2,6$ -glycosidic bond, which had to be user defined. Waters were incorporated using Coot and ARP/wARP. The final models have good stereochemistry and agree very well with the experimental data (Table 1).

Cells, Viruses, and Antibodies

SVG-A cells are a subclone of the human glial cell line SVG transformed with an origin-defective SV40 mutant (Major et al., 1985). SVG-A cells were grown in Minimum Essential Medium supplemented to contain 10% fetal bovine serum (FBS) and penicillin/streptomycin (P/S) (Mediatech, Inc.) in a humidified incubator at 37°C. MAB597 is a hybridoma supernatant that produces a monoclonal antibody against JCV VP1 (Atwood et al., 1995) and was generously provided by Ed Harlow. Penta His Alexa Fluor 488 was used at 10 μ g/mL (QIAGEN). Generation and propagation of the Mad-1/SVE strain of JCV were performed as previously described (Vacante et al., 1989).

Viral Growth and Reinfection Assays

VP1 mutations were generated in the genomic JCV DNA of strain JC12 (Chen and Atwood, 2002), subcloned in puc19 (Gee et al., 2004) with QuikChange (Stratagene) according to the manufacturer's instructions (Table S2), and confirmed by sequencing. Of plasmid DNA, 10 μ g was digested with BamHI (Promega) for 2 hr at 37°C to separate the JCV genomic DNA from the puc19 backbone plasmid. Digests were performed in triplicate for each sample. SVG-A cells were plated to 40% confluence on 18 mm round glass coverslips (Thermo Scientific) in 12-well plates (Costar). Cells in medium without antibiotics were transfected with 2 μ g of digested DNA using Fugene (Roche) at 3:2 ratio (Fugene:DNA). Transfected cells were incubated at 37°C O/N, and medium containing 5% FCS and 2% P/S was added to cells the next day. Cells were incubated at 37°C and fed with 500 μ l of medium containing 5% FBS, 1% P/S, and 1% amphotericin B (Mediatech) or harvested for immunofluorescence at day 4 and at 3 day intervals thereafter for 22 days. For reinfection assays, supernatants were collected at 22 days posttransfection. SVG-A cells at 70% confluence on 22 mm square glass coverslips (Fisher) in 6-well plates (Costar) were infected with 150 μ l of virus supernatant at 37°C for 1 hr, then medium containing 5% FBS, 1% P/S, 1% amphotericin B was added to cells, and cells were incubated at 37°C for 72 hr. Cells were fixed and stained by indirect immunofluorescence.

Indirect Immunofluorescence

Cells were washed in PBS, fixed in cold MeOH, and incubated at -20°C. Cells were washed in PBS, permeabilized with 0.5% TX-100 (USB Corporation) at RT for 15 min, blocked with 10% goat serum (MP Biomedicals)/PBS at RT for 30 min, incubated with VP1-specific antibody MAB597 (1:10) in PBS at 37°C for 1 hr, washed with PBS, incubated with a goat-anti-mouse Alexa Fluor 488 (1:1000) in PBS at 37°C for 1 hr, then washed with PBS. Cells were then mounted on slides using VectaShield with Dapi (Vector Laboratories Inc.). Cells were analyzed for nuclear VP1 staining under a 20 \times objective using an Eclipse 800 or Eclipse TE2000-U microscope (Nikon) equipped with an ORCA-ER digital camera (Hamamatsu).

LSTc Inhibition Assay

JCV (Mad-1/SVE) was pretreated with 5 mM of LSTb or LSTc (V Labs, Inc.) (diluted in sterile diH₂O) in media containing 2% FCS on ice for 1 hr. SVG-A cells in 96-well plates were prechilled at 4°C for 30 min. JCV-LST complexes were added to cells and incubated at 4°C for 1 hr. Cells were washed with PBS twice; media containing 10% FCS, 1% P/S, and 1% amphotericin B was added; and cells were incubated at 37°C for 72 hr. Cells were fixed and stained by indirect immunofluorescence as described above.

Flow Cytometry

Wild-type and mutant JCV VP1 pentamers (100 μ l) in PBS were incubated with SVG-A cells in suspension on ice for 2 hr with occasional agitation. Cells were

washed, pelleted by centrifugation, and suspended in 100 μ l of Penta His Alexa Fluor 488 antibody (QIAGEN) (10 μ g/mL) in PBS on ice for 1 hr. Cells were washed, pelleted, and fixed in 1% paraformaldehyde and analyzed for pentamer binding using a BD FACSCaliber (Benton, Dickinson, and Company) flow cytometer equipped with a 488 nm excitation line. Data were analyzed using BD CellQuestPro (Benton, Dickinson, and Company) and FlowJo (Tree Star, Inc) software.

Statistical Analysis

Means for triplicate samples were compared using an unpaired Student's t test (Microsoft Excel). P values <0.05 were considered statistically significant.

ACCESSION NUMBERS

Coordinates and structure factor amplitudes were deposited with the RCSB data bank (<http://www.rcsb.org/>) under accession codes 3NXD and 3NXG. Structure figures were prepared with PyMol (Schrödinger Inc.).

SUPPLEMENTAL INFORMATION

Supplemental Information includes one figure and two tables and can be found with this article online at doi:10.1016/j.chom.2010.09.004.

ACKNOWLEDGMENTS

We thank members of the Stehle, Atwood, and Feizi laboratories for critical discussion. We also thank the staff at beamlines X06SA and X06DA of the Swiss Light Source (Villigen, CH) for assistance with data collection. This work was funded by the National Institutes of Health (NIH) (Institute of Neurological Disorders and Stroke, NINDS) PPG 1P01NS065719-01A1 (W.J.A. and T.S.), the Deutsche Forschungsgemeinschaft SFB-685 (T.S.), the U.K. Research Councils Basic Technology Grant GR/S79268 "Glycoarrays" (T.F.), Engineering and Physical Research Councils Translational Grant EP/G037604/1 (T.F.), the NCI Alliance of Glycobiologists for Detection of Cancer and Cancer Risk U01 CA128416 (T.F.), the Fundação para a Ciência e Tecnologia SFRH/BPD/26515/2006 (A.S.P.), and Ruth L. Kirchstein National Research Service Awards F32NS064870 (M.S.M.) and F32NS070687 (C.D.S.N.).

Received: April 19, 2010

Revised: July 16, 2010

Accepted: August 17, 2010

Published: October 20, 2010

REFERENCES

- Acquotti, D., Fronza, G., Ragg, E., and Sonnino, S. (1991). Three dimensional structure of GD1b and GD1b-monolactone gangliosides in dimethylsulphoxide: a nuclear Overhauser effect investigation supported by molecular dynamics calculations. *Chem. Phys. Lipids* 59, 107–125.
- Adams, P.D., Afonine, P.V., Bunkoczi, G., Chen, V.B., Davis, I.W., Echols, N., Headd, J.J., Hung, L.W., Kapral, G.J., Grosse-Kunstleve, R.W., et al. (2010). PHENIX: a comprehensive Python-based system for macromolecular structure solution. *Acta Crystallogr. D Biol. Crystallogr.* 66, 213–221.
- Atwood, W.J., Wang, L., Durham, L.C., Amemiya, K., Traub, R.G., and Major, E.O. (1995). Evaluation of the role of cytokine activation in the multiplication of JC virus (JCV) in human fetal glial cells. *J. Neurovirol.* 1, 40–49.
- Breg, J., Kroon-Batenburg, L.M., Strecker, G., Montreuil, J., and Vliegthart, J.F. (1989). Conformational analysis of the sialyl alpha(2-3/6)N-acetylglucosamine structural element occurring in glycoproteins, by two-dimensional NOE 1H-NMR spectroscopy in combination with energy calculations by hard-sphere exo-anomeric and molecular mechanics force-field with hydrogen-bonding potential. *Eur. J. Biochem.* 178, 727–739.
- Campanero-Rhodes, M.A., Smith, A., Chai, W., Sonnino, S., Mauri, L., Childs, R.A., Zhang, Y., Ewers, H., Helenius, A., Imberty, A., et al. (2007). N-glycolyl GM1 ganglioside as a receptor for simian virus 40. *J. Virol.* 81, 12846–12858.

- Carson, K.R., Evens, A.M., Richey, E.A., Habermann, T.M., Focosi, D., Seymour, J.F., Laubach, J., Bawn, S.D., Gordon, L.I., Winter, J.N., et al. (2009a). Progressive multifocal leukoencephalopathy after rituximab therapy in HIV-negative patients: a report of 57 cases from the Research on Adverse Drug Events and Reports project. *Blood* *113*, 4834–4840.
- Carson, K.R., Focosi, D., Major, E.O., Petrini, M., Richey, E.A., West, D.P., and Bennett, C.L. (2009b). Monoclonal antibody-associated progressive multifocal leukoencephalopathy in patients treated with rituximab, natalizumab, and efalizumab: a review from the Research on Adverse Drug Events and Reports (RADAR) Project. *Lancet Oncol.* *10*, 816–824.
- Chen, B.J., and Atwood, W.J. (2002). Construction of a novel JCV/SV40 hybrid virus (JCSV) reveals a role for the JCV capsid in viral tropism. *Virology* *300*, 282–290.
- Cinque, P., Koralknik, I.J., Gerevini, S., Miro, J.M., and Price, R.W. (2009). Progressive multifocal leukoencephalopathy in HIV-1 infection. *Lancet Infect. Dis.* *9*, 625–636.
- Dorries, K. (1998). Molecular biology and pathogenesis of human polyomavirus infections. *Dev. Biol. Stand.* *94*, 71–79.
- Dugan, A.S., Gasparovic, M.L., and Atwood, W.J. (2008). Direct correlation between sialic acid binding and infection of cells by two human polyomaviruses (JC virus and BK virus). *J. Virol.* *82*, 2560–2564.
- Eash, S., Tavares, R., Stopa, E.G., Robbins, S.H., Brossay, L., and Atwood, W.J. (2004). Differential distribution of the JC virus receptor-type sialic acid in normal human tissues. *Am. J. Pathol.* *164*, 419–428.
- Elphick, G.F., Querbes, W., Jordan, J.A., Gee, G.V., Eash, S., Manley, K., Dugan, A., Stanifer, M., Bhatnagar, A., Kroeze, W.K., et al. (2004). The human polyomavirus, JCV, uses serotonin receptors to infect cells. *Science* *306*, 1380–1383.
- Emsley, P., and Cowtan, K. (2004). Coot: model-building tools for molecular graphics. *Acta Crystallogr. D Biol. Crystallogr.* *60*, 2126–2132.
- Ewers, H., Romer, W., Smith, A.E., Bacía, K., Dmitrieff, S., Chai, W., Mancini, R., Kartenbeck, J., Chambon, V., Berland, L., et al. (2010). GM1 structure determines SV40-induced membrane invagination and infection. *Nat. Cell Biol.* *12*, 11–18, Supp. 11–12.
- Feizi, T. (1985). Demonstration by monoclonal antibodies that carbohydrate structures of glycoproteins and glycolipids are onco-developmental antigens. *Nature* *314*, 53–57.
- Feizi, T., Kapadia, A., and Yount, W.J. (1980). I and i antigens of human peripheral blood lymphocytes copop with receptors for concanavalin A. *Proc. Natl. Acad. Sci. USA* *77*, 376–380.
- Freund, R., Garcea, R.L., Sahli, R., and Benjamin, T.L. (1991). A single-amino-acid substitution in polyomavirus VP1 correlates with plaque size and hemagglutination behavior. *J. Virol.* *65*, 350–355.
- Gee, G.V., Tsomaia, N., Mierke, D.F., and Atwood, W.J. (2004). Modeling a sialic acid binding pocket in the external loops of JC virus VP1. *J. Biol. Chem.* *279*, 49172–49176.
- Kabsch, W. (2010). Integration, scaling, space-group assignment and post-refinement. *Acta Crystallogr. D Biol. Crystallogr.* *66*, 133–144.
- Kean, J.M., Rao, S., Wang, M., and Garcea, R.L. (2009). Seroepidemiology of human polyomaviruses. *PLoS Pathog.* *5*, e1000363. 10.1371/journal.ppat.1000363.
- Khalli, K., and White, M.K. (2006). Human demyelinating disease and the polyomavirus JCV. *Mult. Scler.* *12*, 133–142.
- Kishida, S. (2007). Progressive multifocal leukoencephalopathy—epidemiology, clinical pictures, diagnosis and therapy. *Brain Nerve* *59*, 125–137.
- Knowles, W.A., Pipkin, P., Andrews, N., Vyse, A., Minor, P., Brown, D.W., and Miller, E. (2003). Population-based study of antibody to the human polyomaviruses BKV and JCV and the simian polyomavirus SV40. *J. Med. Virol.* *71*, 115–123.
- Komagome, R., Sawa, H., Suzuki, T., Suzuki, Y., Tanaka, S., Atwood, W.J., and Nagashima, K. (2002). Oligosaccharides as receptors for JC virus. *J. Virol.* *76*, 12992–13000.
- Liddington, R.C., Yan, Y., Moulai, J., Sahli, R., Benjamin, T.L., and Harrison, S.C. (1991). Structure of simian virus 40 at 3.8-Å resolution. *Nature* *354*, 278–284.
- Linda, H., von Heijne, A., Major, E.O., Ryschkewitsch, C., Berg, J., Olsson, T., and Martin, C. (2009). Progressive multifocal leukoencephalopathy after natalizumab monotherapy. *N. Engl. J. Med.* *361*, 1081–1087.
- Liu, C.K., Hope, A.P., and Atwood, W.J. (1998a). The human polyomavirus, JCV, does not share receptor specificity with SV40 on human glial cells. *J. Neurovirol.* *4*, 49–58.
- Liu, C.K., Wei, G., and Atwood, W.J. (1998b). Infection of glial cells by the human polyomavirus JC is mediated by an N-linked glycoprotein containing terminal alpha(2-6)-linked sialic acids. *J. Virol.* *72*, 4643–4649.
- Low, J.A., Magnuson, B., Tsai, B., and Imperiale, M.J. (2006). Identification of gangliosides GD1b and GT1b as receptors for BK virus. *J. Virol.* *80*, 1361–1366.
- Major, E.O. (2009). Reemergence of PML in natalizumab-treated patients—new cases, same concerns. *N. Engl. J. Med.* *361*, 1041–1043.
- Major, E.O., Miller, A.E., Mourrain, P., Traub, R.G., de Widt, E., and Sever, J. (1985). Establishment of a line of human fetal glial cells that supports JC virus multiplication. *Proc. Natl. Acad. Sci. USA* *82*, 1257–1261.
- McCoy, A.J., Grosse-Kunstleve, R.W., Adams, P.D., Winn, M.D., Storoni, L.C., and Read, R.J. (2007). Phaser crystallographic software. *J. Appl. Cryst.* *40*, 658–674.
- Murshudov, G.N., Vagin, A.A., and Dodson, E.J. (1997). Refinement of macromolecular structures by the maximum-likelihood method. *Acta Crystallogr. D Biol. Crystallogr.* *53*, 240–255.
- Neu, U., Woellner, K., Gauglitz, G., and Stehle, T. (2008). Structural basis of GM1 ganglioside recognition by simian virus 40. *Proc. Natl. Acad. Sci. USA* *105*, 5219–5224.
- Palma, A.S., Feizi, T., Zhang, Y., Stoll, M.S., Lawson, A.M., Diaz-Rodriguez, E., Campanero-Rhodes, M.A., Costa, J., Gordon, S., Brown, G.D., et al. (2006). Ligands for the beta-glucan receptor, Dectin-1, assigned using “designer” microarrays of oligosaccharide probes (neoglycolipids) generated from glucan polysaccharides. *J. Biol. Chem.* *281*, 5771–5779.
- Pho, M.T., Ashok, A., and Atwood, W.J. (2000). JC virus enters human glial cells by clathrin-dependent receptor-mediated endocytosis. *J. Virol.* *74*, 2288–2292.
- Querbes, W., O’Hara, B.A., Williams, G., and Atwood, W.J. (2006). Invasion of host cells by JC virus identifies a novel role for caveolae in endosomal sorting of noncaveolar ligands. *J. Virol.* *80*, 9402–9413.
- Seth, P., Diaz, F., and Major, E.O. (2003). Advances in the biology of JC virus and induction of progressive multifocal leukoencephalopathy. *J. Neurovirol.* *9*, 236–246.
- Shah, K.V., Fields, B.N., Knipe, D.M., and Howley, P.M. (1996). Third Edition. *Fields Virology, Volume 2* (Philadelphia: Lippincott-Raven Publishers).
- Silverman, L., and Rubinstein, L.J. (1965). Electron microscopic observations on a case of progressive multifocal leukoencephalopathy. *Acta Neuropathol.* *5*, 215–224.
- Stehle, T., and Harrison, S.C. (1997). High-resolution structure of a polyomavirus VP1-oligosaccharide complex: implications for assembly and receptor binding. *EMBO J.* *16*, 5139–5148.
- Stehle, T., Yan, Y., Benjamin, T.L., and Harrison, S.C. (1994). Structure of murine polyomavirus complexed with an oligosaccharide receptor fragment. *Nature* *369*, 160–163.
- Stoll, M.S., and Feizi, T. (2009). Software tools for storing, processing and displaying carbohydrate microarray data. Paper presented at Beilstein Symposium on Glyco-Bioinformatics (Potsdam, Germany: Beilstein Institute for the Advancement of Chemical Sciences).
- Sunyaev, S.R., Lugovskoy, A., Simon, K., and Gorelik, L. (2009). Adaptive mutations in the JC virus protein capsid are associated with progressive multifocal leukoencephalopathy (PML). *PLoS Genet.* *5*, e1000368. 10.1371/journal.pgen.1000368.

Tsai, B., Gilbert, J.M., Stehle, T., Lencer, W., Benjamin, T.L., and Rapoport, T.A. (2003). Gangliosides are receptors for murine polyoma virus and SV40. *EMBO J.* 22, 4346–4355.

Vacante, D.A., Traub, R., and Major, E.O. (1989). Extension of JC virus host range to monkey cells by insertion of a simian virus 40 enhancer into the JC virus regulatory region. *Virology* 170, 353–361.

Van Assche, G., Van Ranst, M., Sciot, R., Dubois, B., Vermeire, S., Noman, M., Verbeeck, J., Geboes, K., Robberecht, W., and Rutgeerts, P. (2005). Progressive multifocal leukoencephalopathy after natalizumab therapy for Crohn's disease. *N. Engl. J. Med.* 353, 362–368.

Varki, A. (2001). Loss of N-glycolylneuraminic acid in humans: Mechanisms, consequences, and implications for hominid evolution. *Am. J. Phys. Anthropol. Suppl.* 33, 54–69.

Wenning, W., Haghikia, A., Laubenberger, J., Clifford, D.B., Behrens, P.F., Chan, A., and Gold, R. (2009). Treatment of progressive multifocal leukoencephalopathy associated with natalizumab. *N. Engl. J. Med.* 361, 1075–1080.

Zurhein, G., and Chou, S.M. (1965). Particles resembling Papova viruses in human cerebral demyelinating disease. *Science* 148, 1477–1479.